1-22-2004

Observations of Overturning in the Upper Mesosphere and Lower Thermosphere

M. F. Larsen
Clemson University

Alan Z. Liu
Embry Riddle Aeronautical University - Daytona Beach, liuz2@erau.edu

C. S. Gardner
University of Illinois at Urbana-Champaign

M. C. Kelley
Cornell University

S. Collins
Cornell University

See next page for additional authors

Observations of overturning in the upper mesosphere and lower thermosphere

M. F. Larsen,[1] A. Z. Liu,[2] C. S. Gardner,[2] M. C. Kelley,[3] S. Collins,[3]
J. Friedman,[4] and J. H. Hecht[5]

Received 22 October 2002; revised 22 September 2003; accepted 15 October 2003; published 22 January 2004.

[1] A number of observations of the sodium density primarily in the mesosphere and lower thermosphere (but also of the electron density structure) have shown what appears to be overturning or convective roll cells near the transition from the mesosphere to the lower thermosphere. The cells are found in the region between 95 and 105 km and occur near the boundary between the region of lower stability in the mesosphere and the region of higher stability in the lower thermosphere. The vertical scale for the rolls is ~5–6 km, and the timescale is ~1–3 hours. The rolls occur in a region characterized by large shear in the neutral winds, but the timescales are too long to be explained by simple Kelvin-Helmholtz instability. We present observations from the University of Illinois lidar facility located at the Starfire Optical Range near Albuquerque, New Mexico, from the Arecibo Observatory in Puerto Rico, and from the Maui/MALT Lidar Facility located on Maui in Hawaii that show the overturning structure. possible mechanisms for generating the convective rolls are discussed, Including the relationship of the observed features to the characteristics expected for an inflection point instability. *INDEX TERMS:* 0341 Atmospheric Composition and Structure: Middle atmosphere—constituent transport and chemistry (3334); 0350 Atmospheric Composition and Structure: Pressure, density, and temperature; 0355 Atmospheric Composition and Structure: Thermosphere—composition and chemistry; *KEYWORDS:* vortex rolls, instabilities, thermosphere

Citation: Larsen, M. F., A. Z. Liu, C. S. Gardner, M. C. Kelley, S. Collins, J. Friedman, and J. H. Hecht (2004), Observations of overturning in the upper mesosphere and lower thermosphere, *J. Geophys. Res.*, *109*, D02S04, doi:10.1029/2002JD003067.

1. Introduction

[2] The importance of instabilities in the dynamics and chemistry of the mesosphere is already clear. Many of the observational and theoretical studies that have been published have focused on the instabilities associated with gravity waves, including convective and dynamical instabilities that result from the growth of wave amplitude with height due to the decreasing background atmospheric density. Notable theoretical studies can be found in the early articles by *Hodges* [1969] and *Lindzen* [1981] who attributed mesospheric turbulence and the associated eddy diffusion to wave saturation and breaking effects. Those papers have been followed by a number of more recent studies that have sought to relate instabilities in vertically propagating waves to the generation of turbulence in the mesosphere. Other observational studies have shown evidence for both convective and dynamical instabilities in connection with gravity wave fluctuations in the mesosphere [see, e.g., *Fritts and Rastogi*, 1985; *Fritts*, 1989; *Bishop et al.*, 2004].

[3] Our goal here is to report observations of what appears to be a common structure in the mesopause region that has not been discussed previously in the literature. Since the structure occurs near 100-km altitude, in a region of the atmosphere where measurements of the neutral atmospheric parameters are difficult to obtain, observations of the phenomenon require special instrumentation or a combination of special instruments. A number of the observations presented here were made with the University of Illinois lidars at the Starfire Optical Range located near Albuquerque, New Mexico, and the Maui/MALT facility located at Haleakala on the island of Maui in Hawaii. Both instruments are sodium lidars with exceptional sensitivity and resolution. We also present other cases observed with the sodium lidar and the 430-MHz incoherent scatter radar at the Arecibo Observatory in Arecibo, Puerto Rico. The primary characteristic of the observed structures is an overturning in the neutral atmosphere over a vertical scale of ~4–6 km near the transition from the mesosphere to the mesopause or lower thermosphere. The timescale associated with the overturning, as seen in the ground-based observations, is ~1–3 hours. The Starfire and Maui/MALT observations were especially important since they provided not only the sodium density structure,

[1]Department of Physics, Clemson University, Clemson, South Carolina, USA.
[2]Department of Electrical and Computer Engineering, University of Illinois, Urbana, Illinois, USA.
[3]School of Electrical Engineering, Cornell University, Ithaca, New York, USA.
[4]Arecibo Observatory, Arecibo, Puerto Rico.
[5]Space and Environmental Technology Center, The Aerospace Corporation, Los Angeles, California, USA.

0148-0227/04/2002JD003067$09.00

Table 1. Beam Directions Used for the Lidar Measurements

Beam	Azimuth	Elevation
1	160.00°	30.48°
2	200.00°	30.48°
3	187.02°	30.48°
4	187.02°	40.48°
5	187.02°	30.75°

which is used to determine the presence of the instability, but also the time history of the temperatures and winds which provides important clues about the mechanisms responsible for generating the overturning.

2. Observations

2.1. Starfire

[4] In October 2000, the Starfire lidar (35°00′N, 106°30′W) was operated in support of the Turbulent Oxygen Mixing Experiment (TOMEX) which included a rocket launch from White Sands Missile Range, as well as other ground-based measurements. The experiment is described in detail in the articles by *Larsen et al.* [2003], *Hecht et al.* [2004], and *Bishop et al.* [2004]. The general characteristics of the lidar instrumentation have been described in the articles by *Grime et al.* [2000], *Liu et al.* [2002], and *Gardner et al.* [2002], for example. In TOMEX, five different beam directions were used, as shown in Table 1. Beam direction 3 was chosen to coincide with the upleg portion of the rocket trajectory. The other pointing directions were distributed about the center beam direction.

[5] The height/time contours of the sodium density observed on 26 October 2000, are shown in the upper righthand panel of Figure 1. The altitude of the layer peak varies with time but has a peak value of approximately 9000 cm^{-3} near 0930 UT at an altitude near 87 km. The feature of interest here is not the peak, however, but the overturning feature that occurs between 0600 and 1000 UT. The bottom of the overturning is located near 95 km around 0800 UT, and the top is near 101 km. The strong upwelling associated with the feature is evident between 0900 and

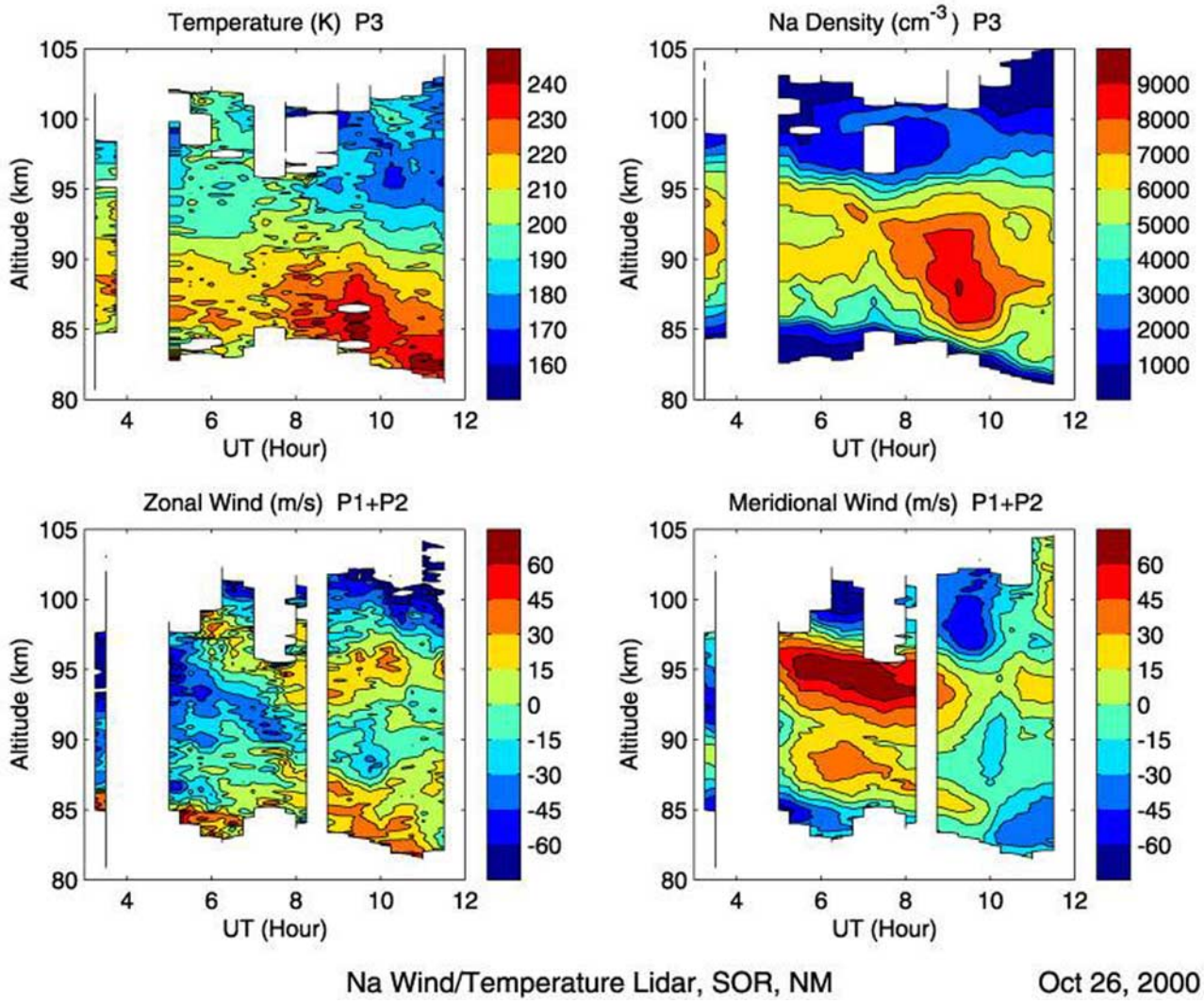

Figure 1. Contours as a function of time and altitude of the temperatures (upper left panel), sodium density (upper right panel), zonal winds (lower left panel), and meridional winds (lower right panel) measured with the Starfire lidar on 26 October 2000.

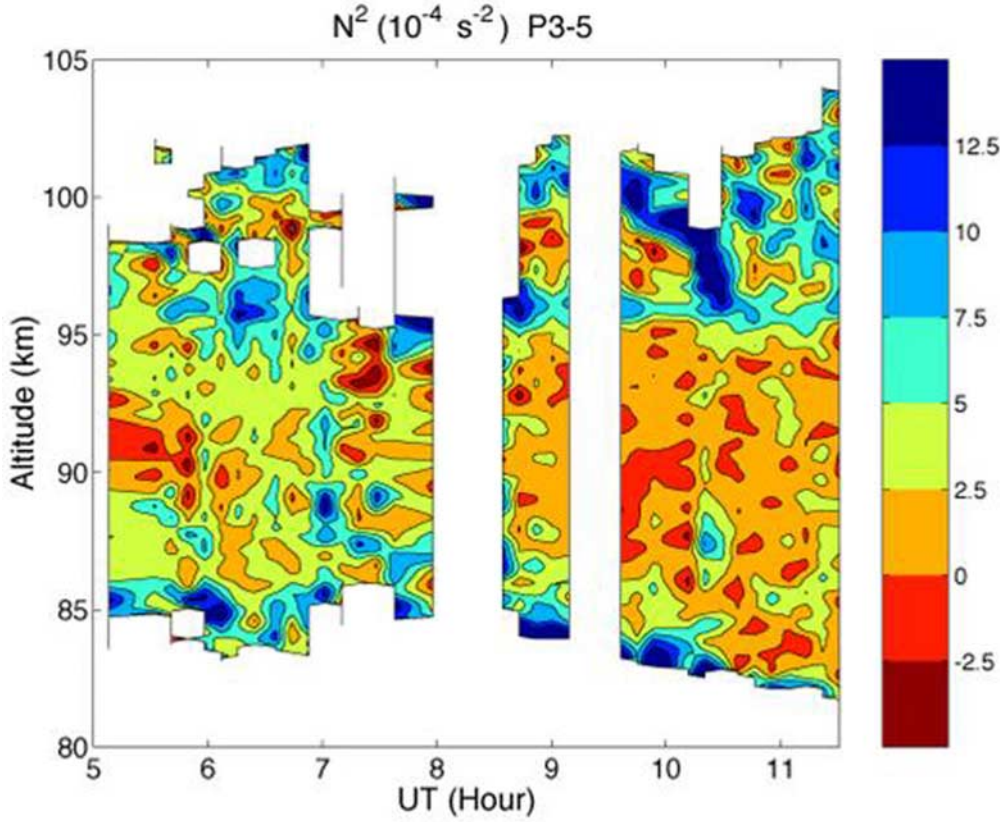

Figure 2. Contours of the Brunt-Väisälä frequencies derived from the lidar temperature measurements on 26 October 2000 as a function of time and altitude.

1000 UT. The top part of the curl extends back to 0600 UT and is represented primarily by the light blue contour (2000–3000 cm^{-3}) during the period. The vertical scale for the feature in this case is 5–6 km, and the timescale is 3–4 hours. The temperatures, zonal winds, and meridional winds measured by the lidar are shown in the upper left, lower left, and lower right hand panels in Figure 1, respectively, for reference.

[6] The contours of the stability, i.e., the square of the Brunt-Väisälä frequencies, calculated from the temperatures measured by the lidar are shown in Figure 2. Between 0700 and 0900 UT, the signal-to-noise ratio is poor between 95 and 100 km altitude so that temperatures could not be determined reliably. Between 0900 and 1000 UT however, the measurements show that the stability is low with N^2 values less than 2.5×10^{-4} s^{-1}. The wind profiles between 95 and 100 km altitude during the time when the overturning is observed have a maximum in the meridional component near 97 km, as shown in the lower right hand panel of Figure 1. A trimethyl aluminum (TMA) chemical release wind profile measurement was made with the rocket that was launched from White Sands Missile Range close to the time of the wind profile shown in Figure 3. The lidar and TMA wind profiles have been compared in detail by *Larsen et al.* [2003] who found excellent agreement between the two sets of measurements.

[7] The Starfire observations thus show an overturning feature with a characteristic timescale of several hours and a characteristic vertical scale of 5–6 km. The region of the overturning is characterized by low stability with temperature decreasing as a function of height in the lower part of the overturning and a region of much higher stability at the top of the feature where the temperature begins to increase rapidly at the base of the thermosphere. The feature occurs in the region of large turning shear just below the large wind maximum in the lower thermosphere. The features of the wind profile shown in Figure 3 are typical of midlatitude wind profiles, as discussed by *Larsen* [2002], who summa-

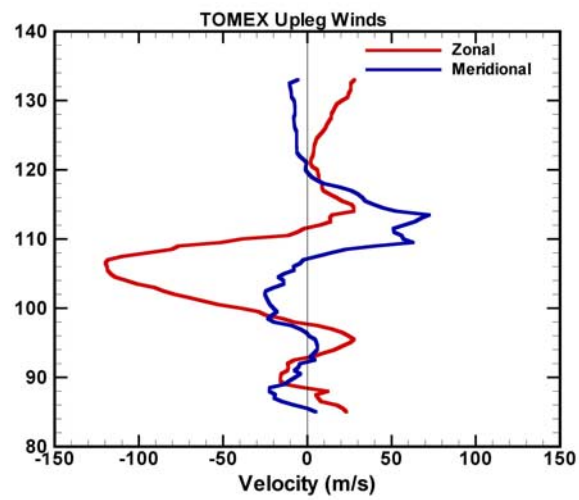

Figure 3. Zonal and meridional wind profiles measured at 1000 UT with the chemical release technique.

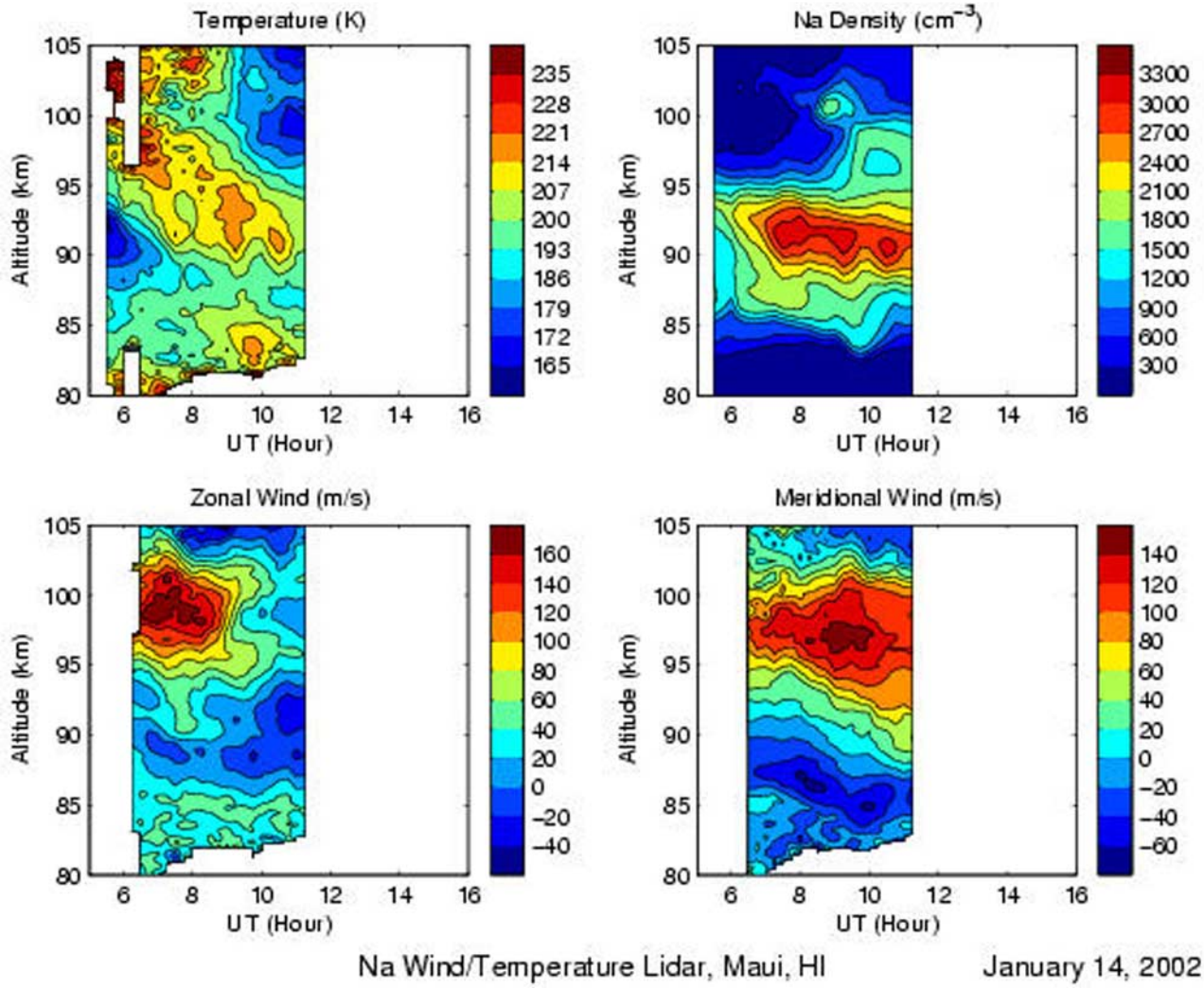

Figure 4. Contours as a function of time and altitude of the temperatures (upper left panel), sodium density (upper right panel), zonal winds (lower left panel), and meridional winds (lower right panel) measured with the Maui/MALT lidar on 14 January 2002.

rized an extensive data set of rocket wind measurement covering over 40 years of observations. The wind profiles show an inflection point in the meridional winds, i.e., a height where the second derivative is zero, near the middle of the height range where the overturning occurs. There is a large shear in the zonal wind in the same altitude range that further decreases the stability.

2.2. Maui / MALT

[8] The first observations with the University of Illinois lidar at the Maui/MALT facility (20°45′N, 156°30′W) were made in January 2002. The capabilities of the instrument are similar to those of the Starfire Optical Range lidar described in the previous section. An example of the overturning observed at the new location is shown in Figure 4. The upwelling associated with the convective roll occurs soon after 1000 UT with the lower part of the feature located near 95 or 96 km. The top of the convective roll is at an altitude near 103 km and extends back to approximately 0700 UT. The duration of the overturning is ~3–4 hours. The temperature contours at 0800 UT, for example, show temperatures decreasing with altitude below 100 km altitude and then increasing above that height. Both the zonal and meridional wind components have large maximum wind speeds that either approach or exceed 150 m s^{-1} between 95 and 100-km altitude.

[9] A second example of a convective roll observed with the Maui lidar is found in Figure 5 which again shows the temperatures, sodium densities, and the zonal and meridional winds. In this case the overturning is shallower than in the previous examples. The upwelling begins near 1130 or 1200 UT around 93–95 km. The top of the overturning is at 98–99 km and extends to the end of the observation period near 1600 UT. In this case the direction of the vortex roll is reversed from that in the previous two examples described above. The observations also show that the convective roll developed after the wind speeds and shears increased in magnitude around 1100 UT.

2.3. Arecibo

[10] In February 1998, the Arecibo Observatory sodium lidar and 430-MHz incoherent scatter radar (18°20′N,

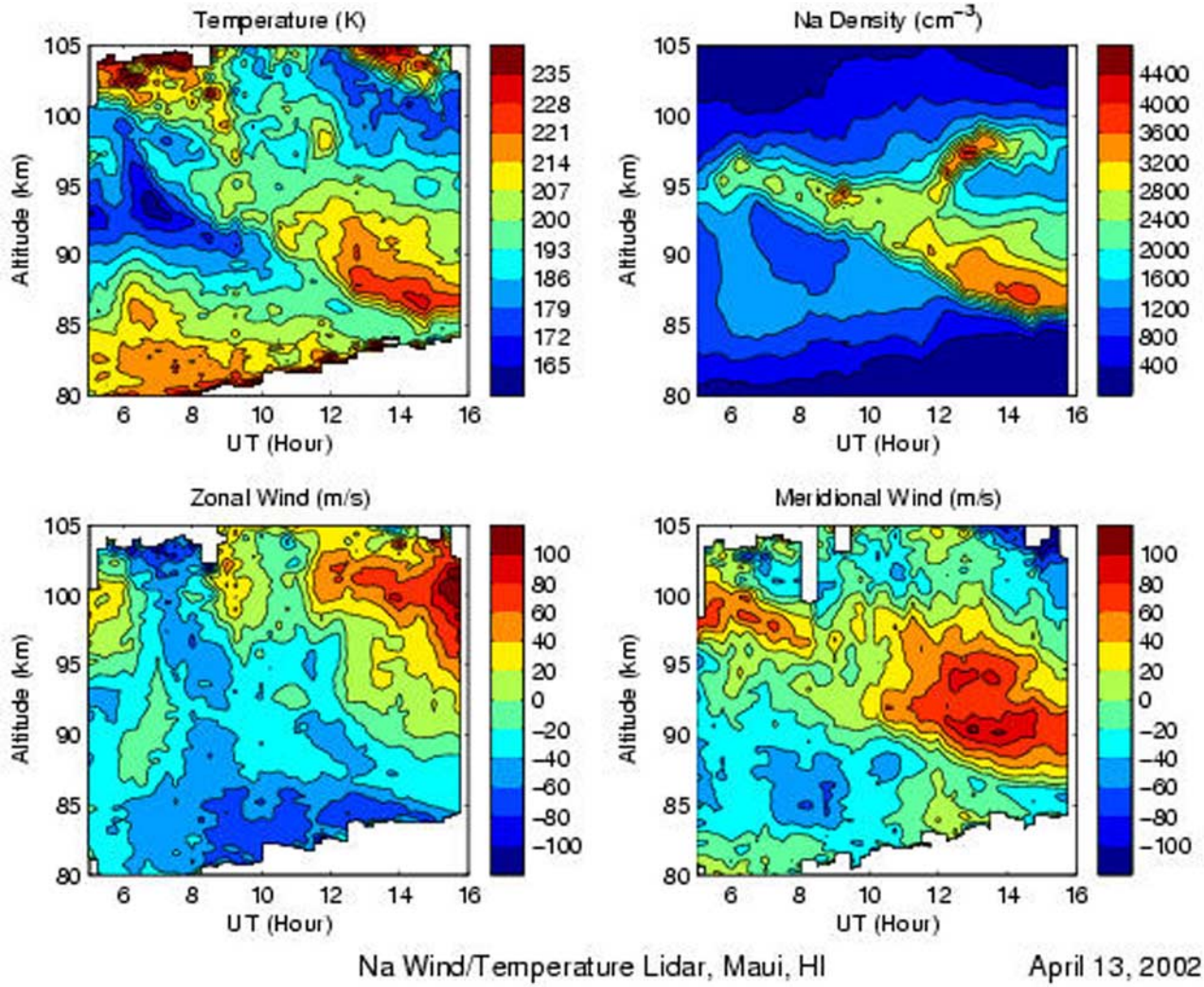

Figure 5. Contours as a function of time and altitude of the temperatures (upper left panel), sodium density (upper right panel), zonal winds (lower left panel), and meridional winds (lower right panel) measured with the Maui/MALT lidar on 13 April 2002.

66°45′W) were both operated extensively in support of the rocket launches carried out at the nearby rocket range located at Tortuguero, Puerto Rico. The Arecibo lidar is much less sensitive than the Starfire lidar, and at the time did not have either temperature or wind measurement capabilities. The Arecibo incoherent scatter radar, on the other hand, has extremely good sensitivity due to the large transmitter power and large receiving antenna size, so that even small perturbations in the electron densities can be observed in the lower *E* region. An example of the data provided by the combination of the two systems is shown in Figure 6. The figure shows the incoherent scatter radar electron density measurements as gray scales overlaid on the lidar sodium density measurements made on the night of 22 February 1998. The lidar measurements are shown by the color shades which are mostly located below 98–99 km. The radar measurements show the curl structure above 99-km altitude between 2100 and 2200 LT. The two sets of measurements together show the upwelling in the neutral sodium that begins close to 2100 LT. The overturning motion is evident in the electron density data from

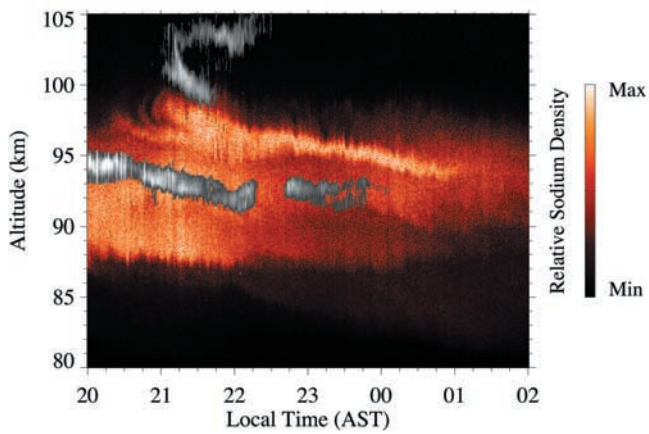

Figure 6. Overlay of the combined sodium lidar and incoherent scatter radar measurements from Arecibo, Puerto Rico, on 22 February 1998. Color shades represent the lidar measurements. Gray shades show the incoherent scatter radar data.

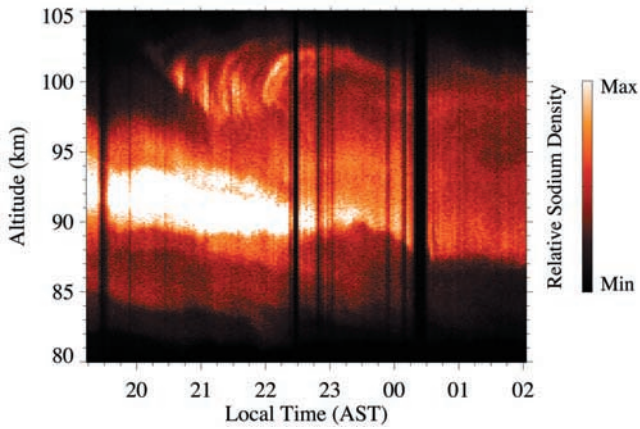

Figure 7. Sodium lidar density measurements from Arecibo, Puerto Rico, on 9 February 1999.

the incoherent scatter radar that extends until 2215 or 2230 LT with the top of the circulation located at 103 or 104-km altitude. The plasma in this case is expected to act more or less as a tracer of the neutral motions. The timescale for the overturning is difficult to determine exactly but is more than one hour, and the vertical scale is from 97 or 98 km to approximately 104 or 105-km altitude, i.e., 6–8 km, which is comparable to the vertical scale of the feature observed in New Mexico. The direction of rotation of the curl in this case is the same as in the 12 April 2002, data from Maui.

[11] Several other examples of the overturning feature were observed during the Puerto Rico observations in 1998 and one in February 1999. Figure 7 shows the sodium lidar density data from the night of 9 February 1999, as a function of local time and altitude. In this case an overturning was clearly evident during the time from approximately 2100 to 0000 LT with several upwelling features prior to the most prominent overturning which begins close to 2200 LT. The entire event covers a period of three hours or more, and the final vortex feature is observed from the ground over a period of almost two hours. The vertical scale is difficult to judge in this case, but the base of the feature appears to be located at 96 or 97 km while the top of the feature is near 102 km, altitudes that are very similar to those observed in the New Mexico event. The sense of rotation is the same as in the previous example.

2.4. Discussion of the Data Sets

[12] The Arecibo data is much more limited than the Starfire data since neither temperature nor wind measurements were available, but the lidar observations show either the upwelling feature or the complete overturning on a number of the nights when the skies were clear and the measurements could be made. The Arecibo incoherent scatter radar has unrivaled sensitivity and, at least on one occasion, showed the extension of the overturning feature to altitudes higher than those where sodium could be detected by the lidar. On other days, the radar showed no discernible structure when the lidar upwellings occurred, but that is not unexpected if the background electron densities in the *E* region were small at the time, as is typically the case in the nighttime *E* region. The Starfire measurements represent a more comprehensive data set with both temperature and wind measurements in addition to the sodium density measurements. The exceptional sensitivity of the lidar makes it possible to detect the small density perturbations associated with the vortex features at higher altitudes above 100 km, although the features were found to be near the limit of detectability even for the Starfire lidar, as shown by the data gaps in Figure 1, for example. The Maui lidar facility provides data that is comparable to that obtained from Starfire. The data from all three sites show features with similar characteristics and located in approximately the same height range in spite of the wide separation in longitude of the three sites. The observations also represent a range of seasons. The measurements are therefore a more or less random sampling that show the frequent occurrence of the convective curls or vortex rolls over a range of seasons and longitudes. The conditions associated with the mechanism or mechanisms responsible for generating the rolls must occur frequently and must explain the observed characteristics, namely that the rolls occur in a localized height range near 100-km altitude, that they have a vertical extent of approximately 3–6 km, and that the periods observed in the earth-fixed frame should be at least one hour or more.

3. Possible Mechanisms for Vortex Roll Generation

3.1. Kelvin-Helmholtz Instability

[13] The convective rolls occur in regions of large shear, suggesting that shear instabilities may be responsible for generating the structures. Overturning or vortex rolls are a common characteristic of Kelvin-Helmholtz instabilities associated with large shears. The features described here are clearly not associated with such instabilities for a number of reasons. Although the shear is large in the part of the atmosphere where the overturning occurs, the region which is unstable in the small Richardson number sense, is localized within a few km in the vertical direction, as discussed in more detail by *Bishop et al.* [2004], and is localized in time as well. The most unstable horizontal wavelength is expected to be approximately 16 km for a shear instability region with a vertical scale of 2 km [see, e.g., *Scorer*, 1997]. The largest shear was in the zonal wind component in the altitude range of interest, so the Kelvin-Helmholtz structures would be aligned approximately in the north-south direction, i.e., perpendicular to the mean wind component. Such structure was indeed observed in the chemical release trail, as described in the article by *Bishop et al.* [2004], but the apparent period produced by such structure advected at a mean velocity of 30 m s^{-1} is 8–10 min which is much less than the period of several hours that is observed. The secondary instabilities associated with the shear instabilities after they become fully developed are aligned with the wind direction [see, e.g., *Palmer et al.*, 1996] and could produce much longer apparent periods in the earth-fixed frame, but the simulations of *Fritts et al.* [1996] have shown that the timescale for such an event, from initial instability to restabilization, is of the order of 30 min, i.e., much shorter than the timescale of the features observed here. The secondary instabilities are therefore an

unlikely explanation since the timescale is too short and the vertical scale of those instabilities is expected to be considerably smaller than the scale that is observed.

3.2. Gravity Wave Breaking

[14] Gravity wave breaking is another possible explanation for the features. The simulations of *Walterscheid and Schubert* [1990] and *Prusa et al.* [1996], for example, show that wave breaking is expected to produce overturning once per wavelength for waves that exceed criticality. Differences between the simulations and the observations presented here include the fact that the wave breaking effects in the model extend over an altitude range of 20 km or more, whereas our observations show features that are very localized in height and that tend to occur near the transition from the mesopause to the lower thermosphere around 100 km. Another difference is that the breaking wave structures produced by the simulations propagate relatively quickly past an observing point on the ground. For example, the structure shown in Figure 1 of the paper by *Walterscheid and Schubert* [1990] moves 10–20 km in approximately 20 min, which is a significant fraction of the wavelength. The details of the solutions will undoubtedly depend on the choice of the incident wave spectrum, and it may well be that the spectrum can be tuned to produce solutions that match the observations more closely, but that is not clear at this point.

3.3. Convective Rolls

[15] An alternative explanation for the observed characteristics of the features described here stems from similarities between conditions in the mesosphere/lower thermosphere transition region and conditions in the planetary boundary layer. Specifically we are interested in possible similarities between the vortex rolls that are commonly observed in the atmospheric boundary layer within the lowest 1–2 km of the atmosphere and the convective rolls that are present in the lidar data. Studies of the convective roll features in the boundary layer have a long history, and the features have been given a number of different names. The earliest observations were of the cloud streets that develop as a consequence of the vortex rolls when sufficient moisture is present. The features themselves have been referred to as boundary layer rolls, vortex rolls, longitudinal instabilities, and organized large eddies. The critical features required to generate them are a region of low stability, i.e., temperature decreasing with altitude, capped by a region of high stability, i.e., temperature increasing with altitude, which is a condition that is also characteristic of the mesosphere/lower thermosphere transition region.

[16] A further requirement is a shear in the background winds. *Brown* [1980] and *Etling and Brown* [1993] have written excellent reviews of the theoretical understanding and the observational data pertaining to the boundary layer vortex rolls. The theoretical papers have focused on longitudinal instabilities. The latter are ultimately inflection point instabilities or generalized shear instabilities, as described in more detail by *Brown* [1972] and *Stensrud and Shirer* [1988], for example, which can exist in both viscid and inviscid flow [see also *Balmforth and Morrison*, 1999]. When an inflection point is present in the flow, the rolls can develop and draw on the energy of the mean flow. The eddy viscosity is clearly an important component of the boundary layer dynamics with a significant influence on the characteristics of the convective roll modes. The angle between the roll axes and the geostrophic wind, for example, is an effect of the eddy viscosity. The eddy diffusion in the altitude range of interest to us is also frequently enhanced below the height of the turbopause, as discussed in the article by *Bishop et al.* [2004] and in a number of the papers cited therein. Breaking gravity waves are the likely to be the drivers for the dynamical processes that lead to the enhanced diffusion, as well as being the drivers of some of the large shears that are observed in the mesosphere/lower thermosphere region.

[17] The paper by *Lilly* [1966] was one of the first to discuss the instability of the Ekman boundary layer wind profile due to the inflection point in the wind profile associated with the rotation of the wind vector with height. His linear analytic treatment clearly indicated that the flow was unstable, but such linear analytic theories have not been particularly successful in predicting the characteristics of the unstable structures, as discussed by *Etling and Brown* [1993]. Stability analysis is complicated because of the dependence on the Reynolds number *Re*, the Rayleigh number *Ra*, the Prandtl number *Pr*, the bulk Richardson number *Ri* and the Rossby number *Ro*. In addition the instability depends on the angle between the mean flow and the roll orientation and on the horizontal wavelength. Numerical modeling studies have been more successful. The results show that aspect ratios of 5–6 are expected, although boundary layer observations have shown aspect ratios as large as 15. The theoretical analyses also show that the vortex rolls are aligned nearly parallel to the mean wind, but with small angles of approximately 10–20° between the wind direction and the axis of the rolls.

[18] In the boundary layer models, the most natural lower boundary condition is a no-slip condition, and the upper boundary condition is often taken as a rigid lid, although the latter may not be realistic. The formulation of the boundary layer problem is therefore treated as a Dirichlet problem. The region of interest for us in the mesopause/lower thermosphere is the altitude range where the winds and wind shears are large (approximately 90–110 km) since the overturning features observed in the sodium density data occur in the region of large winds and shears [*Larsen*, 2002], which are presumed to be the drivers for the observed instabilities. There are no rigid surfaces in the altitude range, but it is clear that the gradients become small outside the region. In fact, the wind speeds also decrease significantly at altitudes below the heights of interest. A reasonable choice of boundary conditions would be to specify the vertical derivatives at the upper and lower boundaries, i.e., to formulate the equations as a Neumann problem. Using the Neumann versus Dirichlet constraints will not change the stability characteristics, although the solution for a specific set of boundary conditions will effectively determine the phasing.

[19] The instabilities can exist in purely turning shear since the requirement is that an inflection point must exist in the profile of one component of the wind. *Brown* [1970] pointed out that, although the initial study by *Lilly* [1966] focused on the instability of the Ekman wind profile, the instability can be produced by other types of forcing that

produce turning shear, such as the thermal wind or, perhaps more appropriately for the mesosphere and lower thermosphere region, the turning shear associated with the tidal motions. As pointed out by *Brown* [1980], instabilities will occur at very moderate velocities if there is an inflection point in the velocity profile. If there are nearly constant flow velocities in two adjacent regions, the transition from one to the other will almost certainly require the presence of an inflection point. The typical background winds in the region of interest for our study are characterized by a rotation of the wind vector with height and an increase in the wind speed with a maximum that usually occurs between 100 and 110-km altitude [*Larsen*, 2002]. The occurrence of an inflection point is therefore highly likely.

[20] For the TOMEX case, the vertical scale of the overturning is approximately 6 km which gives a horizontal scale of 36 to 90 km for the aspect ratios cited above. The differences between the density data from the different beam directions in the TOMEX experiment are small, suggesting that the horizontal scale of the structures is at least many tens of kilometers. For a wind speed of 30 m s^{-1} and a roll axis aligned at an angle of 20° from the mean wind direction, the apparent period in the earth-fixed frame will be between 1 and 2.5 hours, i.e., consistent with the periods found in the data presented here. The parameters in the other observations presented here are comparable to those observed on the TOMEX night. The data that we have included here shows vortex curls in both the clockwise and counterclockwise sense. Since the instability produces counterrotating helical flow in adjacent vortex rolls, both types of rotation can be expected.

4. Discussion

[21] Quantitative conclusions about the frequency of occurrence of the vortex roll structure described here cannot be drawn from the available data which is limited to a few nights, but the fact that they are a common feature in the rather limited data set suggests that the vortex rolls may be a common feature in the mesosphere/lower thermosphere transition region. The measurements include a range of seasons and longitudes and thus represent a more or less random sampling. The mixing produced by the observed overturning is likely to be significant, especially since the vortex rolls occur in a part of the atmosphere where the vertical gradients in the ionization, composition, and winds are large.

[22] The dynamics responsible for the features is not clear. Gravity wave breaking may be a viable explanation for the convective overturning that is observed, especially if the spectrum of incident waves can be fine-tuned to match the observations. An intriguing alternative explanation is that convective roll instabilities may be possible in the mesosphere/lower thermosphere region. In the boundary layer such dynamical features were thought to be infrequent when they were first observed because the rolls were identified mainly on the basis of cloud street observations. Recent observations however, which use radars or lidars, now indicate that the features are a common and important dynamical feature in the boundary layer. In fact, the rolls or large eddies may provide the primary momentum and heat transport in the planetary boundary layer [*Etling and Brown*, 1993]. The conditions required to produce the vortex rolls are common in the boundary layer, namely a low stability region capped by a stable layer, a turning shear with an inflection point, and enhanced eddy diffusion in the low stability region. The same conditions are common in the mesosphere/lower thermosphere transition region and may result in the vortex rolls being a common feature there as well. In the mesosphere, the forcing responsible for the enhanced eddy diffusion and some of the large shears that are observed is likely to be breaking gravity waves, as opposed to the more direct forcing due to the heating that operates in the boundary layer.

[23] Finally, the vortex rolls in the boundary layer often generate a high-speed flow near the top of the rolls. The nocturnal jet, as it is known, is due, at least in part, to the decoupling that results when the flow moves from the highly mixed region associated with the low-stability layer to the less well-mixed region in the high-stability capping layer. The recent article by *Larsen* [2002] has discussed the chemical release wind measurements made over the last four decades which show a tendency for enhanced wind speeds in the 100–110 km altitude range which often have magnitudes of 100–150 m s^{-1}. The increase in the wind speeds in that altitude range is difficult to explain on the basis of any simple tidal or gravity wave breaking theory alone. The vortex rolls may provide a mechanism for generating or enhancing the winds if the rolls are sufficiently common. Further studies of both the occurrence frequency and the dynamics responsible for the features are needed to resolve these questions.

[24] **Acknowledgments.** MFL acknowledges partial support by NASA grants NAG5-5242 and NAG5-5259 and by NSF grant ATM0003168. The Arecibo Observatory is part of the National Astronomy and Ionosphere Center, which is operated by Cornell University under a cooperative agreement with the National Science Foundation.

References

Balmforth, N. J., and P. J. Morrison (1999), A necessary and sufficient instability condition for inviscid shear flow, *Stud. Appl. Math.*, *102*, 309–344.

Bishop, R. L., M. F. Larsen, J. H. Hecht, A. Z. Liu, and C. S. Gardner (1994), TOMEX: Mesospheric and lower thermospheric diffusivities and instability layers, *J. Geophys. Res.*, *109*, D02S03, doi:10.1029/2002JD003079, in press.

Brown, R. A. (1970), A secondary flow model for the planetary boundary layer, *J. Atmos. Sci.*, *27*, 742–757.

Brown, R. A. (1972), On the inflection point instability of a stratified Ekman boundary layer, *J. Atmos. Sci.*, *29*, 850–859.

Brown, R. A. (1980), Longitudinal instabilities and secondary flows in the planetary boundary layer: A review, *Rev. Geophys.*, *18*, 683–697.

Etling, D., and R. A. Brown (1993), Roll vortices in the planetary boundary layer: A review, *Boundary Layer Meteorol.*, *65*, 215–248.

Fritts, D. C. (1989), A review of gravity wave saturation processes, effects, and variability in the middle atmosphere, *Pure Appl. Geophys.*, *130*, 343–371.

Fritts, D. C., and P. K. Rastogi (1985), Convective and dynamical instabilities due to gravity wave motions in the lower and middle atmosphere: Theory and observations, *Radio Sci.*, *20*, 1247–1277.

Fritts, D. C., T. L. Palmer, O. Andreassen, and I. Lie (1996), Evolution and breakdown of Kelvin-Helmholtz billows in stratified compressible flows. Part I: Comparison of two- and three- dimensional flows, *J. Atmos. Sci.*, *53*, 3173–3191.

Gardner, C. S., Y. Zhao, and A. Z. Liu (2002), Atmospheric stability and gravity wave dissipation in the mesopause region, *J. Atmos. Sol. Terr. Phys.*, *64*, 923–929.

Grime, B. W., T. J. Kane, A. Z. Liu, G. Papen, C. S. Gardner, M. C. Kelley, C. Kruschwitz, and J. Drummond (2000), Meteor trail advection observed during the 1998 Leonid shower, *Geophys. Res. Lett.*, *27*, 1819–1822.

Hecht, J. H., A. Z. Liu, R. L. Bishop, J. H. Clemmons, C. S. Gardner, M. F. Larsen, R. G. Roble, G. R. Swenson, and R. L. Walterscheid (2004), An overview of observations of unstable layers during the Turbulent Oxygen Mixing Experiment (TOMEX), *J. Geophys. Res.*, *109*, D02S01, doi:10.1029/2002JD003123, in press.

Hodges, R. R., Jr. (1969), Eddy diffusion coefficients due to instabilities in internal gravity waves, *J. Geophys. Res.*, *74*, 4087–4090.

Larsen, M. F. (2002), Winds and shears in the mesosphere and lower thermosphere: Results from four decades of chemical release wind measurements, *J. Geophys. Res.*, *107*(A8), 1215, doi:10.1029/2001JA000218.

Larsen, M. F., A. Z. Liu, R. L. Bishop, and J. H. Hecht (2003), TOMEX: A comparison of lidar and sounding rocket chemical tracer wind measurements, *Geophys. Res. Lett.*, *30*(7), 1375, doi:10.1029/2002GL015678.

Lilly, D. K. (1966), On the instability of Ekman boundary flow, *J. Atmos. Sci.*, *23*, 481–494.

Lindzen, R. S. (1981), Turbulence and stress owing to gravity wave and tidal breakdown, *J. Geophys. Res.*, *86*, 9707–9714.

Liu, A. Z., W. K. Hocking, S. J. Franke, and T. Thayaparan (2002), Comparison of Na lidar and meteor wind measurements at Starfire Optical Range, NM, USA, *J. Atmos. Sol. Terr. Phys.*, *64*, 31–40.

Palmer, T. L., D. C. Fritts, and O. Andreassen (1996), Evolution and breakdown of Kelvin-Helmholtz billows in stratified compressible flows. Part II: Instability structure, evolution, and energetics, *J. Atmos. Sci.*, *53*, 3192–3212.

Prusa, J. M., P. K. Smolarkiewicz, and R. R. Garcia (1996), Propagation and breaking at high altitudes of gravity waves excited by tropospheric forcing, *J. Atmos. Sci.*, *53*, 2186–2216.

Scorer, R. S. (1997), *Dynamics of Climate and Meteorology*, 686 pp., John Wiley, Hoboken, N. J.

Stensrud, D. J., and H. N. Shirer (1988), Development of boundary layer rolls from dynamical instabilities, *J. Atmos. Sci.*, *45*, 1007–1019.

Walterscheid, R. L., and G. Schubert (1990), Nonlinear evolution of an upward propagating gravity wave: Overturning, convection, transience and turbulence, *J. Atmos. Sci.*, *47*, 101–125.

S. Collins and M. C. Kelley, School of Electrical Engineering, Cornell University, Ithaca, NY 14850, USA. (collins@ee.cornell.edu; mikek@ece.cornell.edu)

J. Friedman, The Arecibo Observatory, HC3 Box 53995, Arecibo, Puerto Rico 00612. (jonathan@naic.edu)

C. S. Gardner and A. Z. Liu, Department of Electrical and Computer Engineering, University of Illinois at Urbana-Champaign, 1308 West Main St., Urbana, IL 61801, USA. (cgardner@uillinois.edu; liuzr@uiuc.edu)

J. H. Hecht, Space and Environmental Technology Center, The Aerospace Corporation, P.O. Box 92957, Los Angeles, CA 90009, USA. (james.h.hecht@aero.org)

M. F. Larsen, Department of Physics, Clemson University, Clemson, SC 29634, USA. (mlarsen@clemson.edu)